Numerical simulation of moving contact line in wetting phenomena using the Generalized Navier Boundary Condition

Nhan T. Le[a], Mathieu Coquerelle[b], Stéphane Glockner[b]

a. Université de Bordeaux, I2M, UMR 5295, France
b. Bordeaux INP, I2M, UMR 5295, France

Abstract

In this paper, we focus on the motion of the interface between two fluids in contact with a solid surface so called the moving contact line problem. Although the Navier-Stokes equations are applicable for fluid flows at micro-scale, the moving interface evolution and surface tension occur at the level of molecules at which the classical mechanics break down. Qian et al. [1] proposed the Generalized Navier Boundary Condition (GNBC) on the basis of molecular dynamics simulation. The GNBC model can eliminate the non-physical singularity in the vicinity of the contact line. Moreover, it can accurately predict the slip condition with small capillary numbers.

We combine GNBC with a macro-micro scale dynamic contact line approach based on Y. Yamamoto et al. [2]. The relation between the macro-micro contact angle is modelized thanks to Cox theory [3]. The evolving and deforming interface is carried within the front tracking framework by J. Glimm et al. [4] and the Navier-Stokes equations are solved by Notus CFD [5] developed at I2M. We show numerical simulation result of capillary rise in tubes that are consistent with theory and experiment. Simulation of a spreading droplet on a surface is also presented and discussed.

Keywords : Moving contact line, generalized Navier boundary condition, front-tracking method, capillary rise, spreading drop.

1 Introduction

The wetting behaviour of liquids on solid surfaces plays an important role in our capacity to understand and validate many multiphase flow phenomena in nature and industry. Examples include insects walking on water and droplet spreading on a leaf. Wetting phenomena are important in technological processes such as ink-jet printing, coating, biological flows, and micro-fluids. The contact line is the intersection between the fluid-fluid interface and a solid wall. In wetting phenomena, the dynamics of the contact line plays an important role. The main purpose of this work is to simulate the dynamic contact line for the capillary rise in tubes and spreading droplets on a solid surface.

In contrast to the well-known Young's relation that representing the static contact line, a theoretical and practical description the dynamic contact line is still an open problem. The difficulty is the inherent multiscale nature of the phenomenon : nanoscale dynamic plays a role on the contact line behavior,

whereas macroscale fluid motion can be described by continuum mechanics. Various models have been proposed to solve this problem such as slip models, lubrication approximations, diffuse interface models, kinetic theory models, and molecular dynamics simulations. There are many reviews on the topic, which gives a more detailed account of the theoretical approaches as well as the vast literature on the subject, see e.g. de Gennes (1985) [6], Bonn et al. (2009)[7] and Snoeije (2013) [8].

We implement a numerical simulation in two dimensions axisymmetric coordinate for two-phase flows of incompressible viscous fluids, including dynamic contact line from microscopic versus macroscopic in a front tracking framework. Thus, we follow a method proposed by Y. Yamamoto et al. [2] which formulated GNBC with the macro-microscopic dynamic contact line by the Cox model. The main idea of this approach is to consider the nondimensional slip parameter, which can be linked to the slip condition with the experimental data. The results show a dynamic wetting which compares well to experiments when the Capillary number is small ($Ca < 0.1$).

Briefly, this paper is structured as follows : the model and the numerical method are discussed in section two and three. Then section four is devoted to the numerical result of capillary rise in tubes and spreading droplet on a surface. Conclusions and future perspectives are drawn in the last section

2 Dynamic contact line model

There are both shreds of evidence from theory analysis, known as the Huh-Scriven's paradox and microscale observations that there exists slip at the two fluids - solid contact line. A common method to regularize this singularity is to establish the slip region wherein the macroscopic equations are still solved while the microscopic effects of the interface can be modified more precisely. Among models in the literature, the Navier slip is widely used. The notion of a Navier slip boundary condition is that the slip velocity is proportional to the shear rate experienced by the fluid on the wall,

$$\beta' u_{slip} = \left.\frac{\partial u}{\partial n}\right|_{wall} \tag{1}$$

where $\partial u/\partial n|_{wall}$ is the shear strain rate at the wall and β' is called the slip length. The value of the slip length depends on the characteristic of the system, such as viscosity and surface roughness. The Navier slip condition is a well-established model to regularize the viscous stress divergence but using it at the contact line is still questionable.

Qian et al. [1] proposed the GNBC from molecular dynamics simulations on immiscible fluid-fluid flows for the diffused interface method. In the GNBC, the amount of slip between the fluids and the solid wall at the contact line is proportional to the sum of tangential viscous stress and the uncompensated Young stress. It relates to the dynamics of the moving contact line at the microscale, as

$$\beta u_{slip} = \tau_{wall}^{visc} + \tilde{\tau}^{Young}. \tag{2}$$

where β is the slip coefficient defined by the energy scale and the range of molecular interaction. The GNBC model can overcome the singularity at the vicinity of the contact line and accurately predicts the slip velocity with many numerical models such as the front tracking method, the immersed boundary-type simulation and the arbitrary Lagrangian-Eulerian framework.

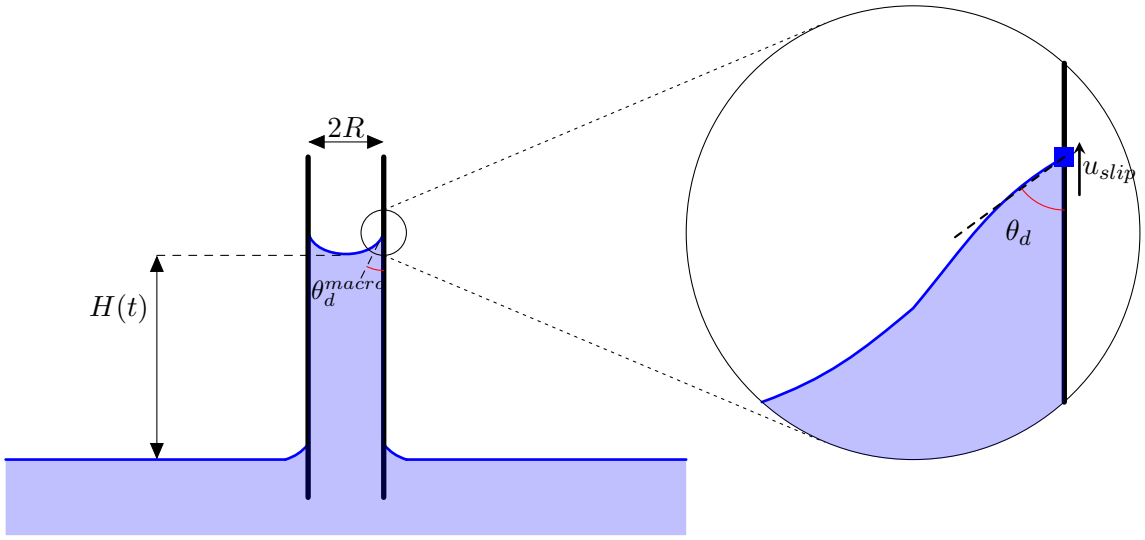

FIGURE 1 – Dynamic contact line in a capillary tube.

In this work, we based on Y. Yamamoto et al. 's approach to modify the GNBC within a front tracking framework. The slip velocity is large at the contact line and the viscous stress is negligible compared to the uncompensated Young stress. The interface is diffused in the parallel direction to the wall, the unbalanced Young's stress is given by the integral

$$\int_{int} \tilde{\tau}^{Young} = \sigma(\cos\theta_s - \cos\theta_d) \tag{3}$$

where σ is the surface tension coefficient, θ_s and θ_d are the microscopic static and the microscopic dynamic contact angle, respectively. The unbalanced Young's stress is discretized at the jth grid point y_j near contact line as

$$\tilde{\tau}^{Young}(y_j) = \sigma(\cos\theta_s - \cos\theta_d)d(y_j - y_{cl}) \tag{4}$$

where y_{cl} is the position of the contact line, and $d(r)$ is the Dirac function proposed by Peskin, $d(r) = \begin{cases} \frac{1}{4\Delta}\left(1 + \cos\frac{\pi r}{2\Delta}\right) & \text{if } |r| \leqslant 2\Delta, \\ 0 & \text{if } |r| > 2\Delta, \end{cases}$ and Δ is the uniform grid spacing. Notice that the amount of slip relates to the deviation of the instantaneous dynamic contact angle is at a microscopic scale as demonstrated by the molecular dynamics simulations. From the nondimensional contact line velocity $Ca = \mu u_{slip}/\sigma$ where μ is the liquid phase viscosity, Eq. 3 with $y = y_{cl}$ and removing τ_{wall}^{visc} in Eq. 2, it follows that :

$$Ca = \chi(\cos\theta_s - \cos\theta_d), \tag{5}$$

where $\chi = \mu/(\beta\Delta)$ is the nondimensional slip parameter that represents the dynamic property of wetting. In reasonable 3D simulations, the dynamic contact angle, however, can be only measured at the macroscopic scale which is the scale of the grid on which the Navier-Stokes equations are solved. The passage from the macro to the micro scale is solved thanks to the relation between the macro-microscopic angle (as in Fig. 1) by Cox-Voinov model :

$$(\theta_d^{macro})^3 = (\theta_d)^3 + 9Ca\ln\left(\frac{l^{macro}}{l^{micro}}\right) + O(Ca), \tag{6}$$

Then θ_d^{macro} can be estimated from the grid-scale angle θ_d^{grid} based on the front tracking representaion with $l^{macro} = \Delta$,

$$(\theta_d^{micro})^3 = (\theta_d^{grid})^3 - 9Ca \ln\left(\frac{\Delta}{l^{micro}}\right). \tag{7}$$

Our procedure at a time level consists of the following steps : first, the interface is advected by Peskin weighted interpolation of the velocity fields. The phase volume and the grid-scale dynamic contact angle θ_d^{grid} are calculated by the marker positions. Then, the densities and viscosities on the grid points are computed through phase volume fraction. The interfacial tension force on the grid points is approximated by Continuum Surface Force model. The microscopic dynamic contact angle and nondimensional contact line velocity Ca are solved from Eq. 7 and 5 by using Newton's iteration method. Finally, the Navier-Stokes and continuity equations are solved with the slip boundary condition.

3 Numerical method

The numerical computations presented herein were performed on an axisymmetric cylindrical coordinate system (x, y) where x and y are respectively the radial (horizontal) and the axial (vertical) directions. The governing equations for mass and momentum can be described in a one-fluid formulation as follows :

$$\begin{aligned} \nabla \cdot \mathbf{u} &= 0, \\ \rho\left(\frac{\partial \mathbf{u}}{\partial t} + \mathbf{u} \cdot \nabla \mathbf{u}\right) &= -\nabla p + \nabla \cdot \left(\mu(\nabla \mathbf{u} + \nabla \mathbf{u}^T)\right) + \rho \mathbf{g} + \mathbf{F}_\sigma, \end{aligned} \tag{8}$$

where $\mathbf{u}$ is the velocity field, p is the pressure, $\mathbf{g}$ is the acceleration due to gravity and $\mathbf{F}_\sigma$ is the surface tension force with the surface tension coefficient σ. For two immiscible fluid flows, the volume fraction C is used to define one of the two phases, C for the liquid and $1 - C$ for the external fluid. Then the other physical properties ϕ such as local density ρ and dynamic viscosity μ are linear function of the phase volume fraction C according to the formula $\phi = C\phi_1 + (1 - C)\phi_2$. The surface tension term is considered to be a force concentrated at the interface $\mathbf{F}_\sigma = \sigma\kappa\delta_\Gamma$ where σ is the surface tension coefficient, κ is the local curvature of the interface, δ_Γ is the Dirac distribution of the interface Γ and $\mathbf{n}$ is the unit outward normal to the interface.

To track explicitly an evolving and deforming interface, we use a front tracking method in a separate Lagrangian interface mesh by a set of connected markers. The interface is made by elements which are linear segments in 2D. The geometric properties, the tangent, the local mean curvature and the contact angle can be directly computed by the coordinate $\mathbf{x}_k$ of markers. Thus , the front tracking interface can precisely describe the phase boundary, capillary forces and contact line angle.

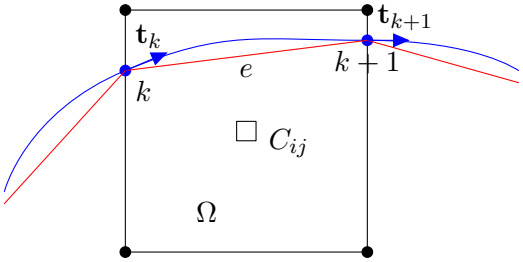

FIGURE 2 – Local force $\mathbf{f}_e$ of element e is computed from tangent $\mathbf{t}_k$ and $\mathbf{t}_{k+1}$ of marker k and $k + 1$.

As in typical balanced force algorithms, the Continuum Surface Force approximation for the surface tension term rewritten relative to the phase volume fraction C :

$$\mathbf{F}_\sigma = \sigma\kappa\nabla\mathbf{C}. \tag{9}$$

where $\nabla\mathbf{C}$ is numerically computed at the faces of the cells. To calculate C for a cell as in Fig. 2, the area of enclosed region Ω is approximated by a polygon. We detect a vertex (x_p, y_p) of the polygon by the intersection of the interface and grid lines or a grid corner. Then the volume of Ω when rotated around y-axis is evaluated by integration.

The interface curvature field $\sigma\kappa$ is calculated following the hybrid formulation introduced by Shin et al. [9] as :

$$\sigma\kappa = \frac{\mathbf{F}' \cdot \mathbf{L}}{\mathbf{G} \cdot \mathbf{G}}, \tag{10}$$

where the discrete numerical expression of the capillary force $\mathbf{F}'$ and $\mathbf{G}$ onto the Eulerian grid are expressed in the form of a sum over elements e of the interface. For example at an $i + 1/2$ cell face

$$\mathbf{F}'_{i+1/2,j} = \sum_e \mathbf{f}_e D_{i+1/2,j}(\mathbf{x}_e)|e|, \tag{11}$$

$$\mathbf{G}_{i+1/2,j} = \sum_e \mathbf{n}_e D_{i+1/2,j}(\mathbf{x}_e)|e|. \tag{12}$$

where $\mathbf{f}_e$ is the capillary force contribution of element e and $D_{i+1/2,j}(\mathbf{x}_e)$ is the Dirac distribution function approximated by

$$D_{i+1/2,j}(\mathbf{x}_e) = \frac{1}{\Delta x \Delta y} d\left(\frac{x_{i+1/2,j} - x_e}{\Delta x}\right) d\left(\frac{y_{i+1/2,j} - y_e}{\Delta y}\right) \tag{13}$$

The total tension force acting on a interface element e in 2D is calculated following :

$$\mathbf{f}_e = \int_e \sigma\kappa\mathbf{n}ds = \sigma(\mathbf{t}_{k+1} - \mathbf{t}_k). \tag{14}$$

where $\mathbf{t}_k$ and $\mathbf{t}_{k+1}$ are the tangent vectors at markers k and $k+1$ shown in Fig. 2 that define the interface element e. For the axisymmetric coordinate system, the axisymmetric interface field on Eulerian gird is calculated by distributing the local axisymmetric curvature of the interface markers in form

$$\kappa^{axis}_{i+1/2,j} = \sum_k \kappa^{axis}_k D_{i+1/2,j}(\mathbf{x}_k) / \sum_k D_{i+1/2,j}(\mathbf{x}_k) \tag{15}$$

where $\kappa^{axis}_k = n_x/x_k$, n_x : the radial component of interface normal $\mathbf{n}$ as $x_k \neq 0$ and $\kappa^{axis}_k = \kappa^{2D}_k$ as $x_k = 0$. Then the effect of circumferential component was add to Eq. 9

$$\mathbf{F}_\sigma = \sigma\left(\kappa^{2D} + \kappa^{axis}\right)\nabla\mathbf{C}, \tag{16}$$

The interface markers are advected in Lagrangian grid by the following equation

$$\frac{d\mathbf{x}_k}{dt} = \mathbf{v}_k. \tag{17}$$

using the Euler method where the velocity $\mathbf{v}$ of marker k is given by the Peskin weighted interpolation

of velocity field from Eulerian grid by

$$\mathbf{v}_k = \sum_{i,j} \mathbf{u}_{ij} D_{i,j}(\mathbf{x}_k) \Delta x \Delta y. \tag{18}$$

Once the interface has been advected, a redistribution of the markers is carried on to optimize the homogeneous distribution of points along the interface.

We used FronTier library package to track the dynamic motion of explicit interface and Notus flow solver for our numerical simulation. Time discretization of the momentum equation is a first order Euler scheme with an implicit formulation for the viscous term. The velocity/pressure coupling under the incompressible flow constraint is solved with the time splitting pressure correction method of Goda. The equations are discretized on a staggered grid by means of the finite volume method. The space derivatives of the inertial term is discretized by a first-order upwind scheme.

4 Simulations of wetting phenomena

4.1 Capillary rise in tubes

We simulate a flow rising in a capillary tube to study the detailed behavior of the dynamic contact line. Gas and glycerin 50 water are used for simulation. The boundary conditions, initial liquid height, and fluids properties are the same as those in Yamamoto et al. [2]. The axisymmetric simulation geometry of this test is a vertical rectangle with size $R \times 40R$, where $R = 0.512$ (mm) is the radius of the capillary tube. The number of grid points are set at $N = 16$ and $N = 32$ per tube radius. Then a time step of 10^{-6}(s) is used and satisfied the capillary time step constraint. The static contact angle is $37.08°$.

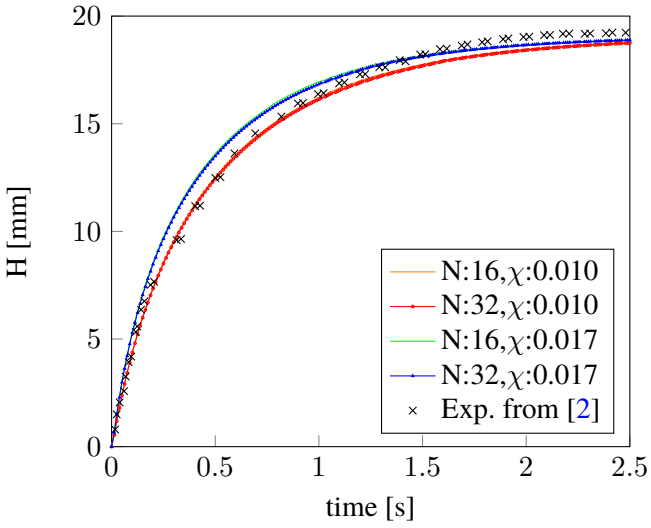

FIGURE 3 – Liquid column height with time.

The evolution of liquid height is shown in Fig. 3. In this case, we use the adjusted parameters ($\chi = 0.017, 0.01$ and $l^{micro} = 10^{-9}$ (m) to determine the micro-dynamic contact line. The height of the liquid is nearly the same as experiment [2]. We observed that the result is not mesh dependent solution as shown by Yamamoto et al. The Fig. 4 shows the relation between contact line velocity and dynamic contact angle. It suggests that the micro dynamic contact angle is also linearly dependent on slip velocity. That agrees with experimental results.

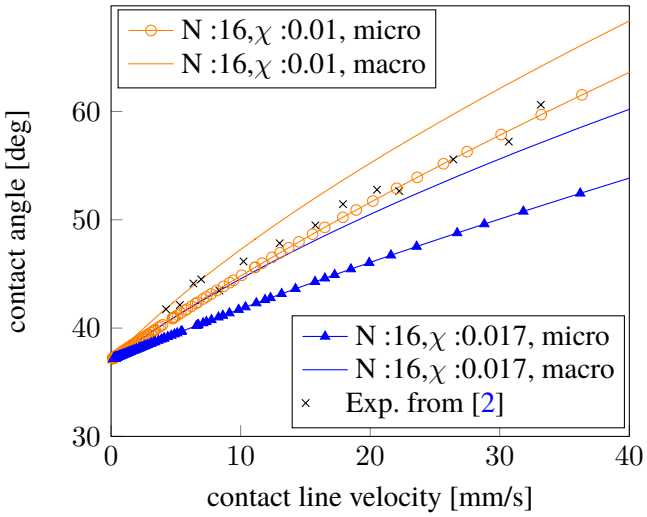

FIGURE 4 – Relation between dynamic contact angle and contact line velocity

4.2 Spreading of a droplet on a solid surface

Simulation was performed for water and gas, with equilibrium contact angle $90°$. The physical parameters and non-dimensional numbers for the two liquids according to Yokoi et al. [11]. The axisymmetric domain is the square with size 5mm $\times$ 5mm. The Neumann boundary condition is set to the top and right boundary, the symmetric boundary is set to the left and the bottom is the wall on which the GNBC is applied. The initial droplet has radius $R = 1.14$ mm and impacts to the wall with initial velocity 1 m/s.

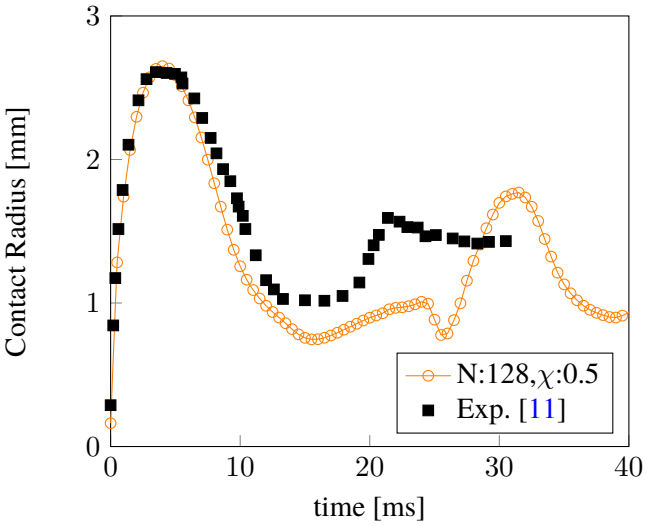

FIGURE 5 – Spreading radius as a function of time.

Fig. 5 shows the spreading radius of the droplet during the impact. The number of grid points is 128×128 for the simulation and the time step is 4×10^{-6}. The slip length is set to 10^{-9} (m) and the nondimensional slip parameter is set to 0.5 based on S. Shin et al. 's model [12]. Our result reproduced the first advancing phase of contact line the same as the experiment. Then the evolution of spreading radius during the receding flow is also close (but a bit slower) to the experiment up to a time equal to $10ms$. The equilibrium state between $12ms$ to $18ms$ is not well reproduced and some discrepancies appear further. There may

be several causes that are under consideration. First of all, a simulation with a finer mesh should be run to confirm - or not - the observed behavior. In the article of Shin et al. [12], a mesh of 256×256 is used, but also a different modelisation of the contact angle that relies upon advancing/receding contact angle to fit better to the experiment. The proposed work is a first attempt to use for the droplet test case the GNBC and the Cox model as defined by Yamamoto et al. One can notice that the viscous stress at the wall is neglected, which may be discussed for the drop impact test case. Finally, the need for more accurate numerical methods is another point on which we are working since we have noticed that the redistribution of the markers made in the Frontier library has a strong impact on the stability of the flow.

5 Conclusion

We have presented in this work simulations of wetting phenomena based on a macro-micro approach. For the rising flow in the capillary tube, our result is consistent with experiment and other numerical simulation. The spreading droplet simulation only well describes the advancing phase and part of the receding phase up to the first equilibrium state. Discrepancies appear that may have several causes. Further works are needed and will help to conclude if the proposed approach - that does not use experimental advancing/receding macroscopic contact angle - can reproduce correctly the drop impact up to the final equilibrium state.

Références

[1] T. Qian, X.-P. Wang, and P. Sheng, Molecular scale contact line hydrodynamics of immiscible flows, *Phys. Rev. E*, vol. 68, no. 1, 016306, Jul. 2003.

[2] Y. Yamamoto, K. Tokieda, T. Wakimoto, T. Ito, and K. Katoh, Modeling of the dynamic wetting behavior in a capillary tube considering the macroscopic–microscopic contact angle relation and generalized Navier boundary condition, *International Journal of Multiphase Flow*, vol. 59, pp. 106–112, 2014.

[3] R. G. Cox, The dynamics of the spreading of liquids on a solid surface. Part 1. Viscous flow, *Journal of Fluid Mechanics*, vol. 168, no. 1, p. 169, 1986.

[4] J. Du, B. Fix, J. Glimm, et al., A simple package for front tracking, *Journal of Computational Physics*, vol. 213, no. 2, pp. 613–628, Apr. 2006.

[5] M. Coquerelle, S. Glockner, A fourth-order accurate curvature computation in a level set framework for two-phase flows subjected to surface tension forces, *Journal of Computational Physics*, vol. 305, pp. 838–876, 2016.

[6] P. G. de Gennes, Wetting : statics and dynamics, *Reviews of Modern Physics*, vol. 57, no. 3, pp. 827–863, Jul. 1985.

[7] D. Bonn, J. Eggers, J. Indekeu, J. Meunier, and E. Rolley, Wetting and spreading, *Reviews of Modern Physics*, vol. 81, no. 2, pp. 739–805, May 2009.

[8] Jacco H. Snoeijer and Bruno Andreotti. Moving Contact Lines : Scales, Regimes, and Dynamical Transitions, *Annual Review of Fluid Mechanics*, vol. 45, no. 1, pp. 269–292, Jan. 2013.

[9] S. Shin, S. I. Abdel-Khalik, V. Daru, and D. Juric, Accurate representation of surface tension using the level contour reconstruction method, *Journal of Computational Physics*, vol. 203, no. 2, pp. 493–516, 2005.

[10] W. Ren and W. E, Boundary conditions for the moving contact line problem, *Physics of Fluids*, vol. 19, no. 2, 022101, 2007.

[11] K. Yokoi, D. Vadillo, J. Hinch, I. Hutchings, Numerical studies of the influence of the dynamic contact angle on a droplet impacting on a dry surface, *Physics of Fluids*, vol 21, 072102, 2009.

[12] S. Shin, J. Chergui, D. Juric, Direct simulation of multiphase flows with modeling of dynamic interface contact angle, *Theor. Comput. Fluid Dyn.*, vol. 32, no. 5, pp. 655–687, 2018.